LA-UR-23-23647

Approved for public release; distribution is unlimited.

Title:	Terrain-Influenced Winds and Fire-Fire Interactions in Wildland Fire Simulations
Author(s):	Robinson, David Joseph
Intended for:	PhD Defense Presentation
Issued:	2023-04-18 (rev.1)

Los Alamos NATIONAL LABORATORY

Terrain-Influenced Winds and Fire-Fire Interactions in Wildland Fire Simulations

David Robinson

April 10th, 2023

LA-UR-23-23647

Wildland Fire Prevalence and Cost

Wildfires

Year	Number of Fires	Number of Acres Affected
2022	68,988	7,577,183
2021	58,985	7,125,643
2020	58,950	10,122,336
2019	50,477	4,664,364
2018	58,083	8,767,492

https://www.nifc.gov/fire-information/statistics/wildfires

Prescribed Fire

Year		BIA	BLM	USFS	FWS	NPS	State/Other	Total
2019	Fires	340	195	3,103	579	176	177,155	151,542
	Acres	77,637	74,786	1,232,145	227,835	209,223	4,236,882	6,058,508
2018	Fires	289	201	3,076	668	148	445,953	450,335
	Acres	82,387	58,307	1,313,182	264,274	161,676	4,481,149	6,360,975
2017	Fires	247	188	2,323	586	138	198,952	202,434
	Acres	89,330	77,134	958,264	178,394	183,029	4,943,229	6,429,229
2016	Fires	240	315	3,061	757	214	78,418	83,005
	Acres	99,712	64,454	1,284,277	266,769	79,881	2,220,418	4,015,511

https://www.nifc.gov/fire-information/statistics/prescribed-fire

Suppression Costs

	Forest Service	DOI Agencies	Total
5 year average	$2,336,084,200	$526,800,000	$2,862,884,200
10 year average	$1,897,153,100	$461,450,700	$2,358,603,800

https://www.nifc.gov/fire-information/statistics/suppression-costs

Damages

"U.S. wildfire damages in 2020 totalled $16.5 billion, ranking it as the third-costliest year on record, behind 2017 ($24 billion) and 2018 ($22 billion)."

https://yaleclimateconnections.org/2021/01/reviewing-the-horrid-global-2020-wildfire-season/

HIGRAD/FIRETEC

- Models temperature, buoyancy, emissions, and fuel consumption.
- Captures complex wind-fire interactions in 3D fuel structure.

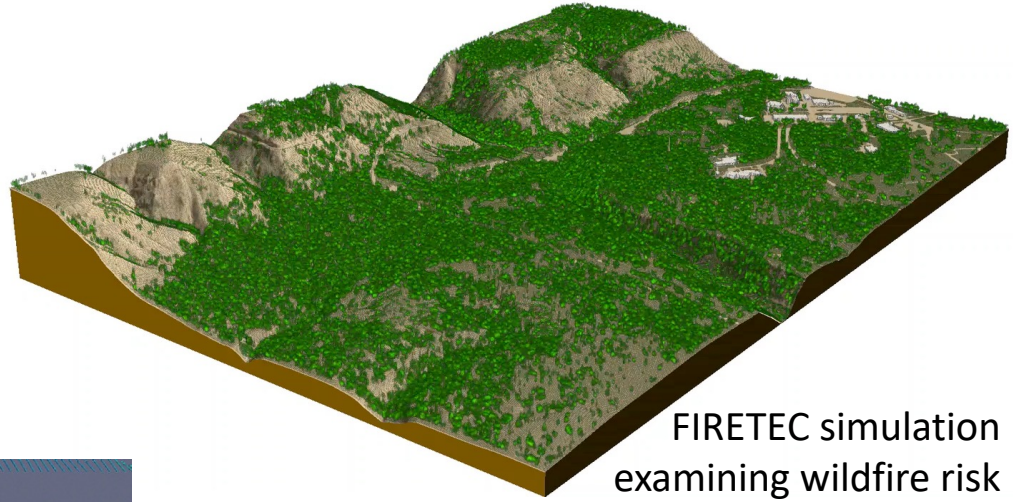

FIRETEC simulation examining wildfire risk

FIRETEC simulation of fire burning in homogeneous fuels

Colors indicate streamwise velocity-component magnitudes:

(red towards the viewer and blue is away from the viewer)

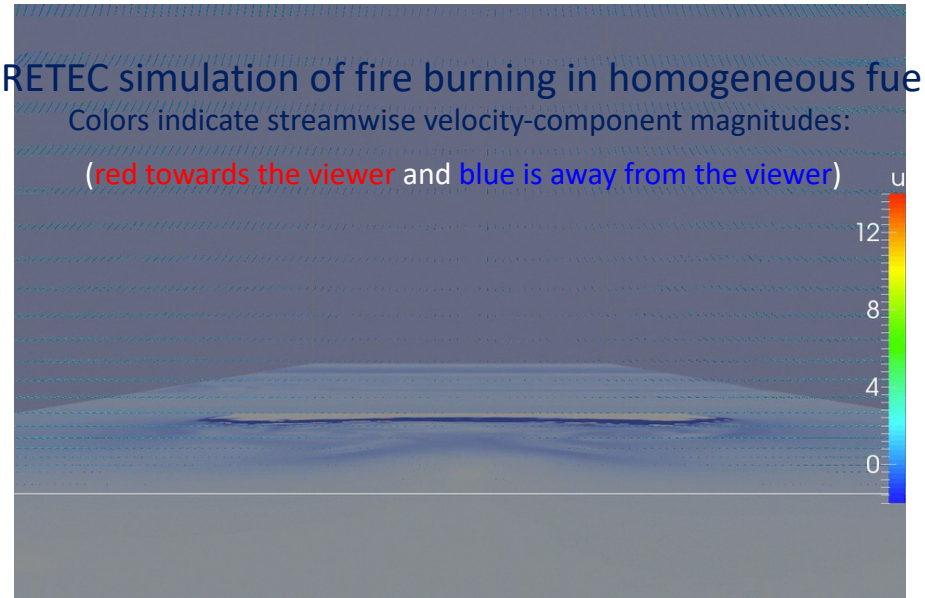

QUIC-Fire

- 3D fuel and wind fields.
- Buoyant plume model.
- Tracks emissions.
- Low Computational Cost.
- Fast Running.

But…

Originally designed for modelling fire on flat ground.

3 x Moisture

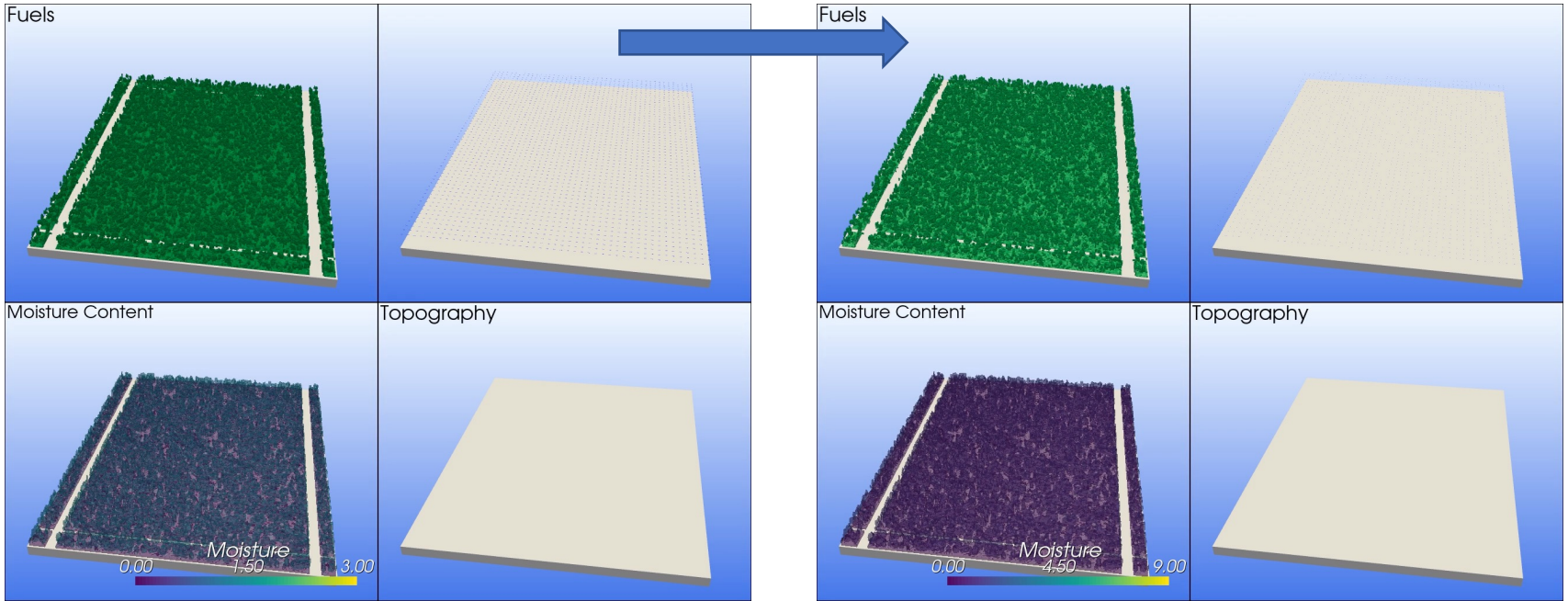

Outline

1. Transformation of QUIC-URB to terrain-following coordinates.

2. Integration of terrain-following QUIC-URB into QUIC-Fire.

3. Modification of QUIC-URB wind solver.

QUIC-URB Overview

1. Take an initial wind field $\tilde{\mathbf{u}}_0 = (\tilde{u}_0, \tilde{v}_0, \tilde{w}_0)$
   - Typically initialized as log or power law profile using a sensor measurement.
2. Inject wake eddy parameterizations.
   - Based on wind speed and geometries of buildings.
3. Calculate mass-conserved wind field.

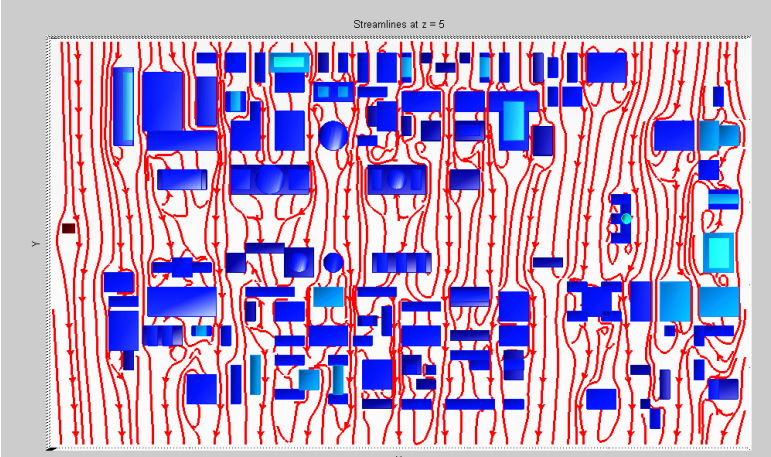

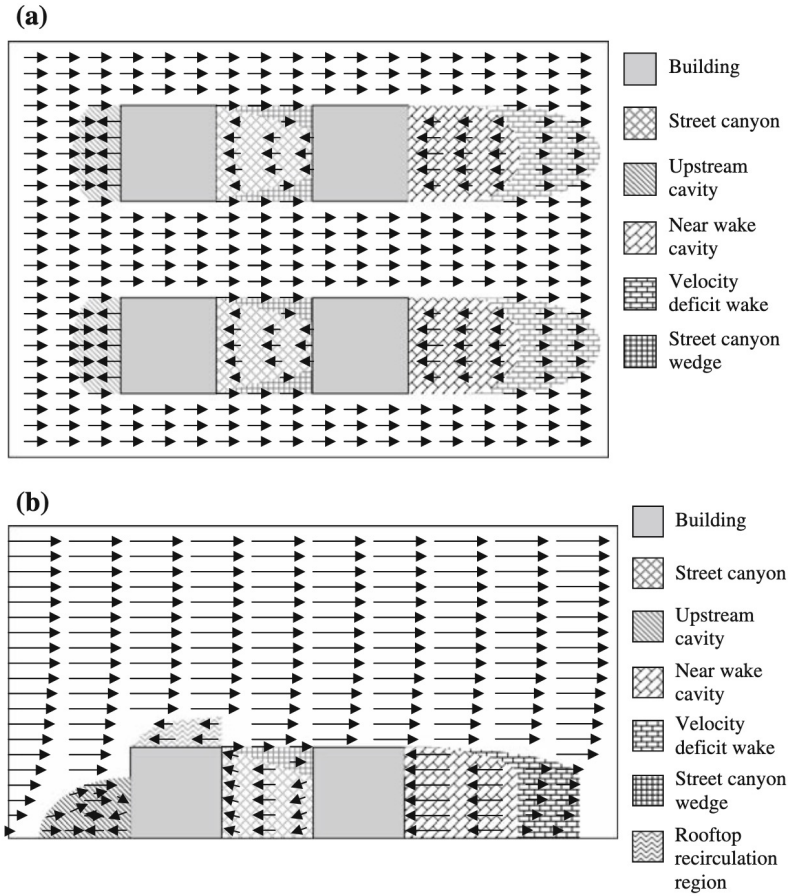

Singh et al. (2008)

QUIC-URB Overview (How)

No Momentum

$$E(\widetilde{u},\widetilde{v},\widetilde{w},\lambda)=\int_V\left[\alpha_1^2(\widetilde{u}-\widetilde{u}_0)^2+\alpha_1^2(\widetilde{v}-\widetilde{v}_0)^2+\alpha_2^2(\widetilde{w}-\widetilde{w}_0)^2+\lambda\nabla\cdot\vec{v}\right]d\widetilde{x}d\widetilde{y}d\widetilde{z}$$

- Minimize Integral
  - Face-centered velocities
  - Cell-centered Lagrange Multipliers
  - α_1 and α_2 are Gaussian precision moduli (weight importance of initial winds)
- Euler-Lagrange Equation
  - Solution is the minimum of integral (nearby mass-conserved velocity field)
- Finite difference discretization results in linear system of equations solved via Successive Over-Relaxation (SOR)

$$\nabla^2\lambda=-2\alpha_1^2\nabla\cdot\widetilde{\mathbf{u}}_0,$$

$$\widetilde{u}=\widetilde{u}_0+\frac{1}{2\alpha_1^2}\frac{\partial\lambda}{\partial\widetilde{x}},$$

$$\widetilde{v}=\widetilde{v}_0+\frac{1}{2\alpha_1^2}\frac{\partial\lambda}{\partial\widetilde{y}},$$

$$\widetilde{w}=\widetilde{w}_0+\frac{1}{2\alpha_2^2}\frac{\partial\lambda}{\partial\widetilde{z}}.$$

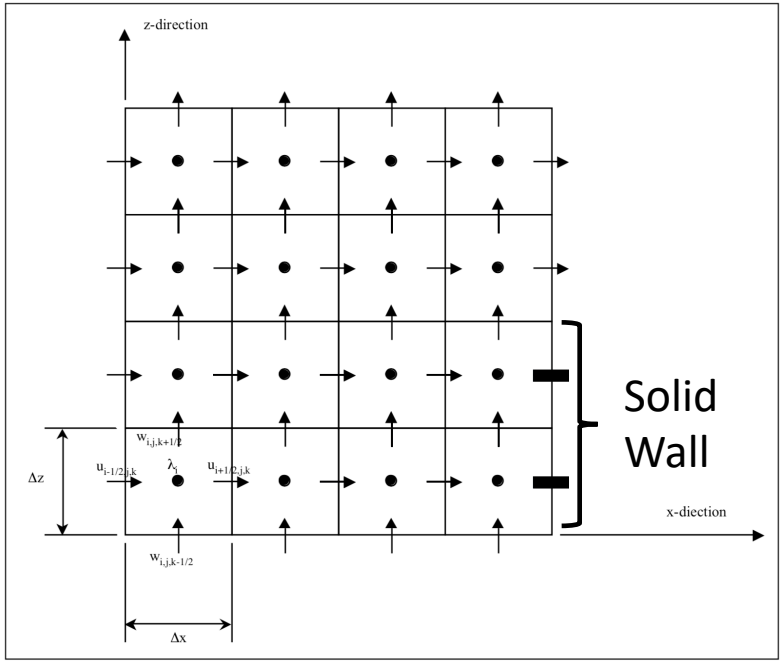

QUIC-URB Grid

QUIC-URB → Terrain-Following Coordinates

- Derivation of the terrain-following form.
- A look at two test cases. (Simple and complex terrain)
  - What it gets right and what it gets wrong.
- Published: David Robinson et al. “QUIC-URB and QUIC-fire Extension to Complex Terrain: Development of a Terrain-Following Coordinate System.” In: Environmental Modelling & Software 159 (2023), p. 105579. doi: 10.1016/j.envsoft.2022.105579.

Block-Cartesian

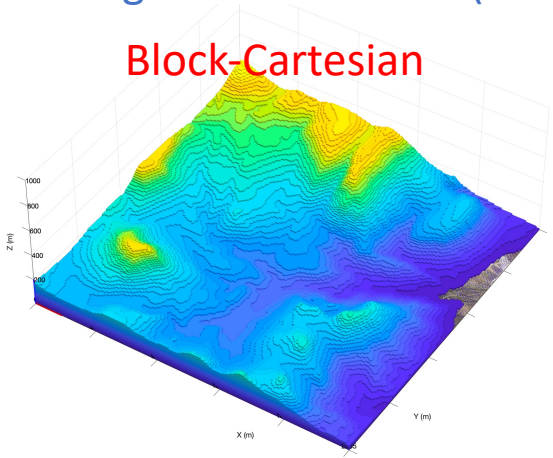

Terrain-Following

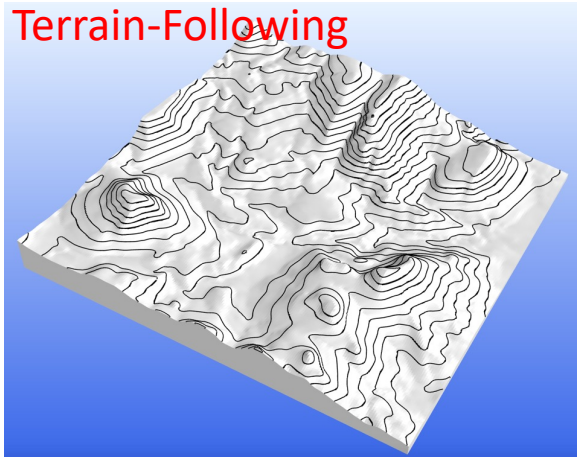

Terrain-Following QUIC-URB

- Terrain-Following (σ) Coordinates

$$x = \widetilde{x},$$
$$y = \widetilde{y},$$
$$z = H\frac{\widetilde{z} - h(\widetilde{x},\widetilde{y})}{H - h(\widetilde{x},\widetilde{y})}$$

Given

H : Domain Height

$h(\widetilde{x},\widetilde{y})$: Terrain Height

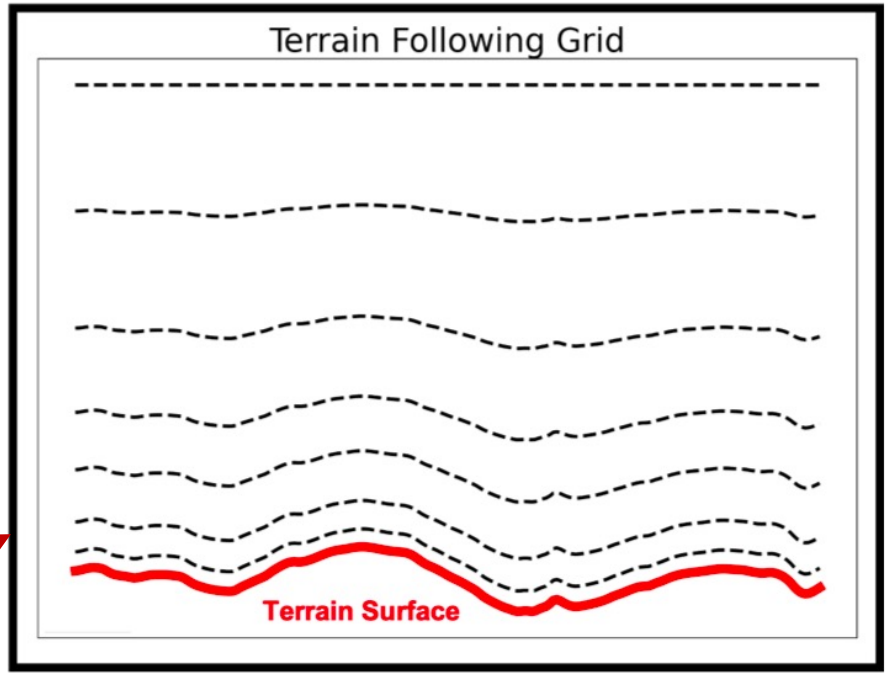

- C

Solving for cartesian z results in the terrain-following grid

$e^1 = i,\ e^2 = j,$ and

$$U^i = \left(\widetilde{u}\vec{i} + \widetilde{v}\vec{j} + \widetilde{w}\vec{k}\right)\cdot e^i \quad \Rightarrow \quad U^1 = \widetilde{u},\ U^2 = \widetilde{v},$$

$$e^3 = h_x\frac{z-H}{H-h}\vec{i} + h_y\frac{z-H}{H-h}\vec{j} + \frac{H}{H-h}\vec{k}.$$

$U^3_{z=0} = 0$ results in $\langle \widetilde{u}, \widetilde{v}, \widetilde{w} \rangle$ that is parallel to terrain surface

$$U^3 = \widetilde{u}h_x\left(\frac{z-H}{H-h}\right) + \widetilde{v}h_y\left(\frac{z-H}{H-h}\right) + \widetilde{w}\left(\frac{H}{H-h}\right).$$

1 ial derivatives of the respective direction (i.e., $h_x = \partial h/\partial x$).

Robinson et al. (2023)

Terrain-Following QUIC-URB

$$E\left(\widetilde{u},\widetilde{v},\widetilde{w},\lambda\right)=\int_V\left[\alpha_1^2\left(\widetilde{u}-\widetilde{u}_0\right)^2+\alpha_1^2\left(\widetilde{v}-\widetilde{v}_0\right)^2+\alpha_2^2\left(\widetilde{w}-\widetilde{w}_0\right)^2+\lambda\nabla\cdot\vec{v}\right]d\widetilde{x}d\widetilde{y}d\widetilde{z}$$

- Contravariant Divergence

$$\nabla\cdot\mathbf{U}=\frac{\partial U^1}{\partial x}+\frac{\partial U^2}{\partial y}+\frac{\partial U^3}{\partial z}-\left(\frac{1}{H-h}\right)\left(U^1h_x+U^2h_y\right)$$

- Substitute contravariant terms into integral.

$$E(U^1,U^2,U^3,\lambda)=\int_V L\left(U^1,U^2,U^3,\frac{\partial U^1}{\partial x},\frac{\partial U^2}{\partial y},\frac{\partial U^3}{\partial z},\lambda\right)d\mathbf{x}.$$

When (15) is at its minimum energy, then

$$\frac{\partial L}{\partial f}-\sum_{j=1}^{3}\frac{\partial}{\partial X^j}\left(\frac{\partial L}{\partial f_j'}\right)=0,\quad \boxed{f_j'=\frac{\partial f}{\partial X^j}},$$

where $f=\left(U^1,U^2,U^3,\frac{\partial U^1}{\partial x},\frac{\partial U^2}{\partial y},\frac{\partial U^3}{\partial z},\lambda\right)$ is any of the dependent variables.

Calculate terms using Euler-Lagrange Equation

Contravariant Form

$$\begin{aligned}E(U^1,U^2,U^3,\lambda)=\int_V\Bigg[&\alpha_1^2\left(U^1-U_0^1\right)^2+\alpha_1^2\left(U^2-U_0^2\right)^2\\&+\alpha_2^2\Bigg\{\left(U^3-U_0^3\right)\left(\frac{H-h}{H}\right)\\&+\left[\left(U^1-U_0^1\right)h_x+\left(U^2-U_0^2\right)h_y\right]\left(\frac{H-z}{H}\right)\Bigg\}^2\\&+\lambda\left(\frac{\partial U^1}{\partial x}+\frac{\partial U^2}{\partial y}+\frac{\partial U^3}{\partial z}\right.\\&\left.-\left(\frac{1}{H-h}\right)\left(U^1h_x+U^2h_y\right)\right)\Bigg]d\mathbf{x},\end{aligned}\qquad(15)$$

Robinson et al. (2023)

Terrain-Following QUIC-URB

- From Euler-Lagrange Equation:

$$U^1 - U_0^1 = \frac{1}{2\alpha_1^2}\left[\lambda_x - \lambda_z\left(\frac{H-z}{H-h}\right)h_x\right],$$
$$U^2 - U_0^2 = \frac{1}{2\alpha_1^2}\left[\lambda_y - \lambda_z\left(\frac{H-z}{H-h}\right)h_y\right],$$
$$U^3 - U_0^3 = \frac{1}{2\alpha_2^2}\lambda_z\left(\frac{H}{H-h}\right)^2 - \frac{1}{2\alpha_1^2}\left(\frac{H-z}{H-h}\right)\left[h_x\lambda_x + h_y\lambda_y - \lambda_z\left(\frac{H-z}{H-h}\right)\left(h_x^2+h_y^2\right)\right],$$

and the continuity equation

$$U_{0,x}^1 + U_{0,y}^2 + U_{0,z}^3 - \left(\frac{1}{H-h}\right)\left(U^1 h_x + U^2 h_y\right) = 0.$$

Differentiate

Substitute

Rearrange

$$\lambda_{xx}+\lambda_{yy}+\left[\left(\frac{z-H}{H-h}\right)^2\left(h_x^2+h_y^2\right)+\eta\left(\frac{H}{H-h}\right)^2\right]\lambda_{zz} + 2\left(\frac{z-H}{H-h}\right)\left[h_x\lambda_{xz}+h_y\lambda_{yz}\right] + \left(\frac{z-H}{H-h}\right)\left[h_{xx}+h_{yy}+\frac{2}{H-h}\left(h_x^2+h_y^2\right)\right]\lambda_z = -2\alpha_1^2\nabla\cdot\mathbf{U}_0, \quad (20)$$

Contravariant Equivalent of: $\nabla^2\lambda = -2\alpha_1^2\nabla\cdot\tilde{\mathbf{u}}_0$

Robinson et al. (2023)

Terrain-Following QUIC-URB

- Discretize Derivatives (mostly central-difference)

$$\lambda_x\Big|_{i,j,k} \approx \frac{\lambda_{i+1,j,k} - \lambda_{i-1,j,k}}{2\Delta x}, \quad \lambda_{xx}\Big|_{i,j,k} \approx \frac{\lambda_{i+1,j,k} - 2\lambda_{i,j,k} + \lambda_{i-1,j,k}}{\Delta x^2}, \quad \frac{\partial \lambda}{\partial z}\Big|_{i,j,k-0.5} \approx \frac{\lambda_{i,j,k} - \lambda_{i,j,k-1}}{z_{m,k} - z_{m,k-1}},$$

$$\lambda_{xz}\Big|_{i,j,k} = \frac{\partial}{\partial z}\left(\frac{\partial \lambda}{\partial x}\right)\Big|_{i,j,k} \approx \frac{1}{\Delta z_k}\left(\frac{\partial \lambda}{\partial x}\Big|_{i,j,k+0.5} - \frac{\partial \lambda}{\partial x}\Big|_{i,j,k-0.5}\right).$$

$$\frac{\partial \lambda}{\partial x}\Big|_{i,j,k-0.5} \approx \frac{1}{\Delta z_{m,k-1}}\Big[(z_{m,k} - z_k)\,\lambda_x|_{i,j,k} + (z_k - z_{m,k-1})\,\lambda_x|_{i,j,k-1}\Big]$$

- No-Flow Bottom Boundary Condition:
  - Initialize $U^3_{z=0} = 0$
  - Enforce $U^3 - U^3_0 = 0$ at $z = 0$

    using $U^3 - U^3_0 = \frac{1}{2\alpha_2^2}\lambda_z\left(\frac{H}{H-h}\right)^2 - \frac{1}{2\alpha_1^2}\left(\frac{H-z}{H-h}\right)\left[h_x\lambda_x + h_y\lambda_y - \lambda_z\left(\frac{H-z}{H-h}\right)(h_x^2 + h_y^2)\right],$
  - Resulting in: $\lambda_z = \frac{h_x\lambda_x + h_y\lambda_y}{\left(\frac{H}{H-h}\right)(\eta + h_x^2 + h_y^2)}$

Robinson et al. (2023)

Terrain-Following QUIC-URB

- Discretizing bottom BC results in $\lambda_{k=1} = \lambda_{k=2} - \frac{\Delta z_{m,k=1}}{\left(h_x^2 + h_y^2 + \eta\right)\left(\frac{H}{H-h}\right)} \left[\frac{h_x}{4\Delta x}\left(\lambda_{i+1,k=2} - \lambda_{i-1,k=2} + \lambda_{i+1,k=1} - \lambda_{i-1,k=1}\right) + \frac{h_y}{4\Delta y}\left(\lambda_{j+1,k=2} - \lambda_{j-1,k=2} + \lambda_{j+1,k=1} - \lambda_{j-1,k=1}\right)\right]$

- Vertical velocities above surface set to $w_0 = -\frac{H-z}{H-h}\left(h_x u_0 + h_y v_0\right)$ (equivalent to $\widetilde{w} = 0$)
  - Generates initial divergence in the field in the presence of terrain. (motivated by Ross et al. 1988)

$$\lambda'_{i,j,k} = \frac{\sum_{i^*=i-1}^{i+1}\sum_{j^*=j-1}^{j+1}\sum_{k^*=k-1}^{k+1} C_{i^*,j^*,k^*}\lambda_{i^*,j^*,k^*}}{D_{i,j,k}} - \frac{2\alpha_1^2\left(\nabla\cdot\mathbf{U}_0\right)_{i,j,k}}{D_{i,j,k}} \quad \text{for } (i^*,j^*,k^*) \neq (i,j,k), \quad (26)$$

General Form

- Set $\lambda^0_{i,j,k} = 0$ and iterate $\lambda^{(\ell+1)}_{i,j,k} = (1-\omega)\lambda^{(\ell)}_{i,j,k} + \omega\lambda'_{i,j,k}$ until $\frac{\epsilon^{(\ell)}}{\epsilon^1} \leq 0.001,$

where $\epsilon^{(\ell)} = \frac{\sum_{i,j,k}\left|\lambda^{(\ell)}_{i,j,k} - \lambda^{(\ell-1)}_{i,j,k}\right|}{n_{\text{cells}}}$, and $\lambda'_{i,j,k}$ includes λ from iteration ℓ and $\ell+1$.

Robinson et al. (2023)

Case: Askervein Hill (Simple Terrain)

- Data provided by MF03-D and TU03B datasets from Taylor and Teunissen (1987)
  - Sensors along three transects.
    - Transect A has wind direction measurements.
  - Dataset used for evaluation of a similar model. Forthofer et al. (2014)
- Minimal vegetation

- 6 km x 6 km x 0.76 km domain
  - 257 x 257 x 18 cells
  - Reference sensor located 3 km upwind
  - Background wind aligned perpendicular to ridge.

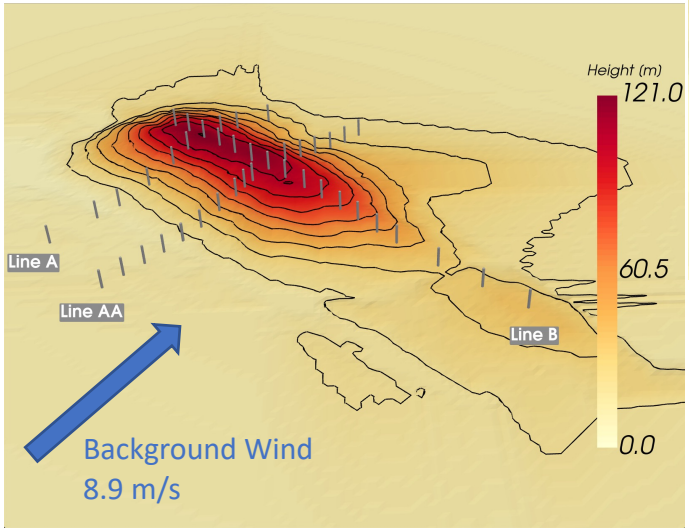

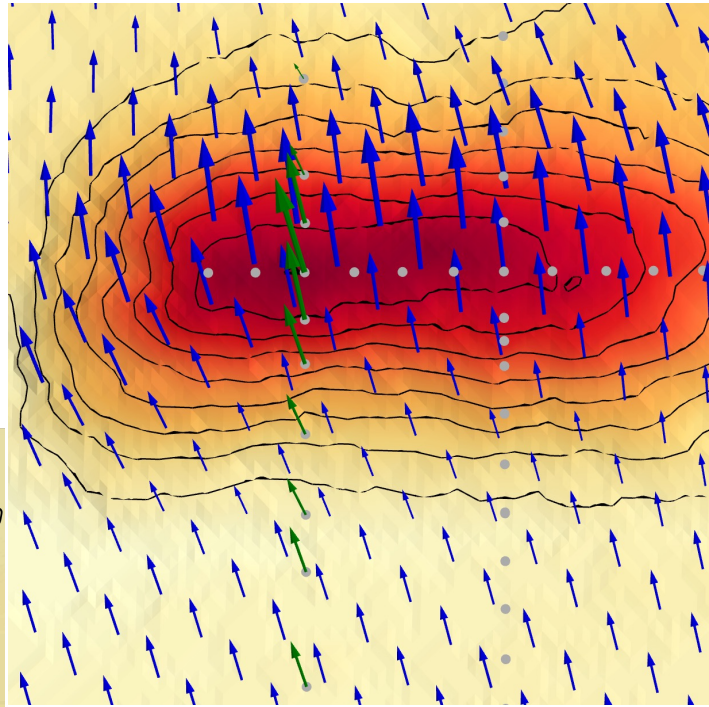

Sensor Winds Model Winds

Robinson et al. (2023)

Askervein Hill: Errors

Robinson et al. (2023)

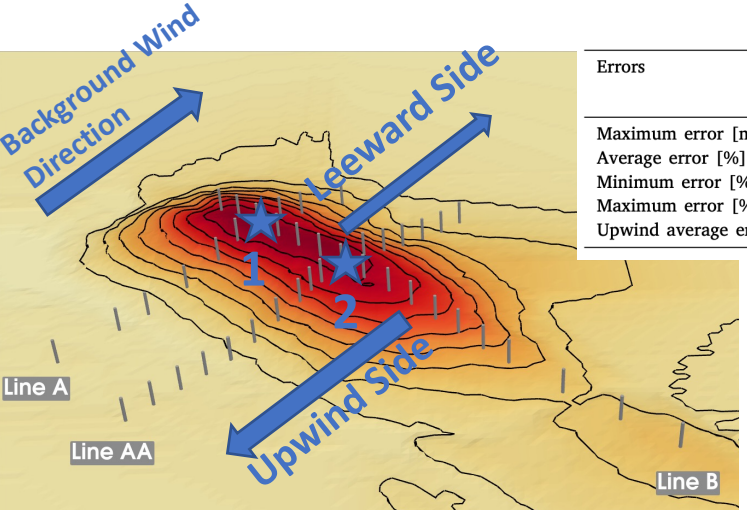

Errors	Transect		
	A	AA	B
Maximum error [ms^{-1}]	5.09	2.58	2.96
Average error [%]	28.4	13.5	5.67
Minimum error [%]	0.02	0.81	0.19
Maximum error [%]	137.5	47	22
Upwind average error [%]	6.83	3.63	N/A

- 6 seconds to compute on laptop

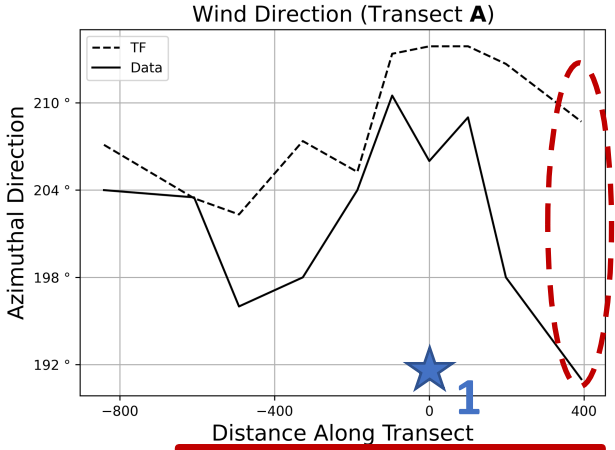

Max Direction Error

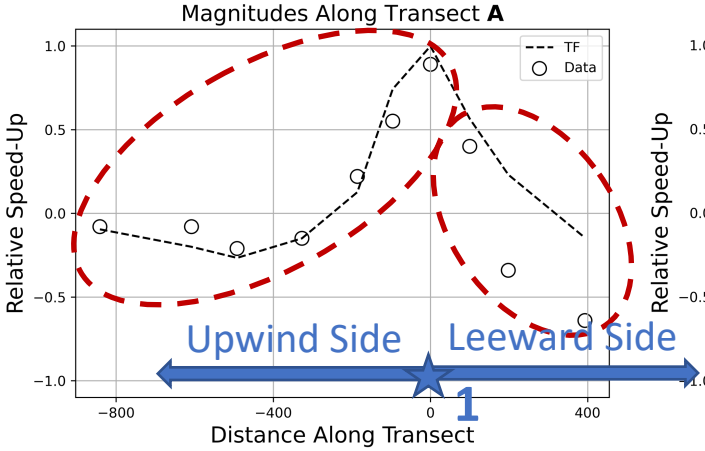

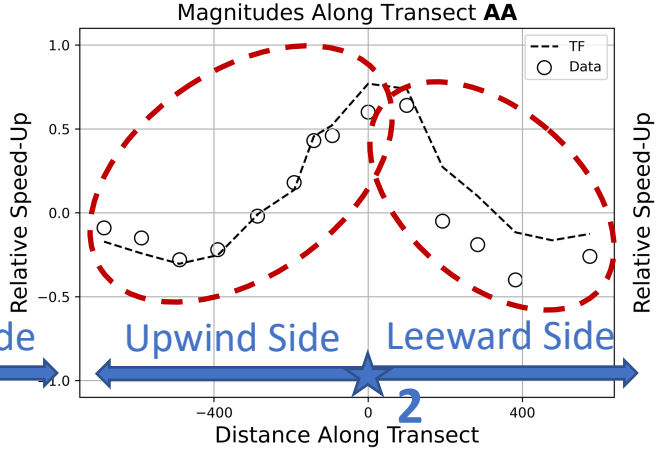

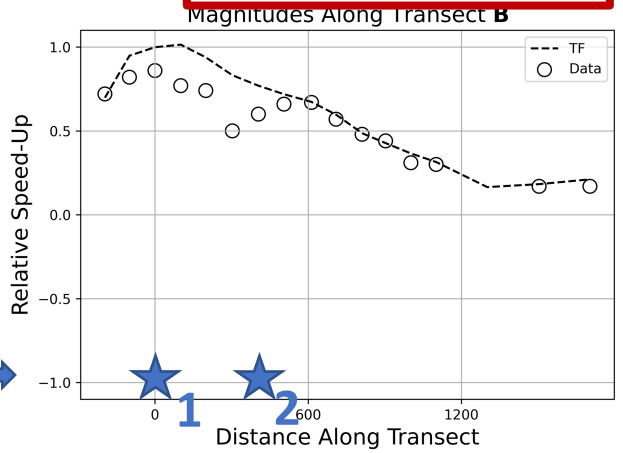

Robinson et al. (2023)

Complex Terrain Case: Socorro Mountains

- 2019 field experiment recorded winds using:
  - 11 2D sonic anemometers
  - 2 ZephIR Lidars
  - 5 3D sonic anemometers
- Most sensors located within 2.25 km x 2.25 km region.

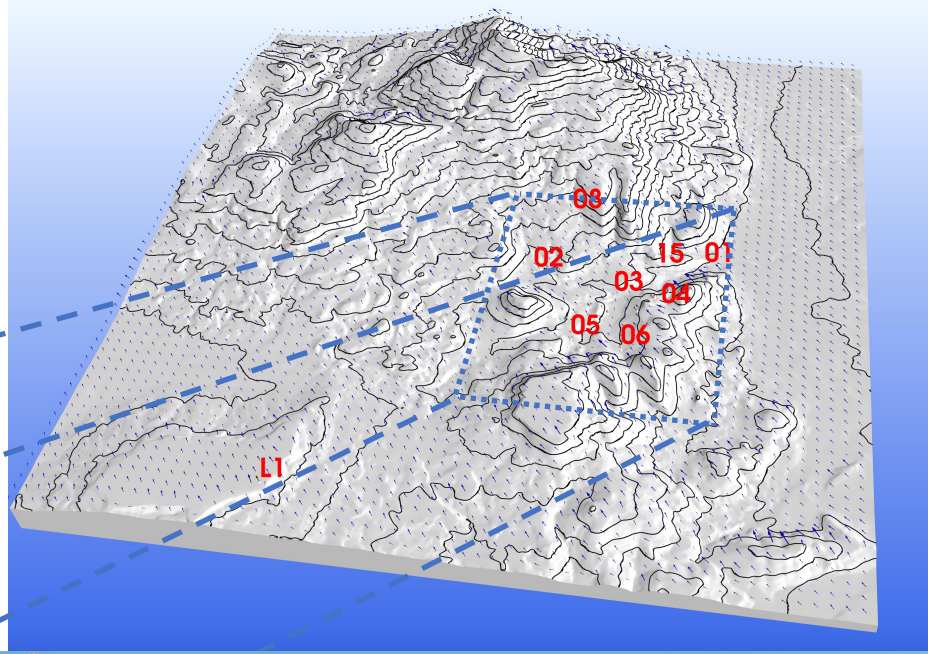

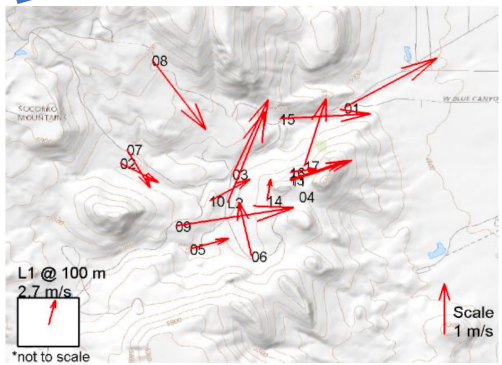

Socorro Mountains Simulation Domain

- 4-10 Hz sensor data ➡ 10 minute averages
- Domain: 2.25 km x 2.25 km x 1 km
- 11 m x 11 m topography resolution
- 205 x 205 x 38 cells
- L1 lidar sensor used to initialize background winds

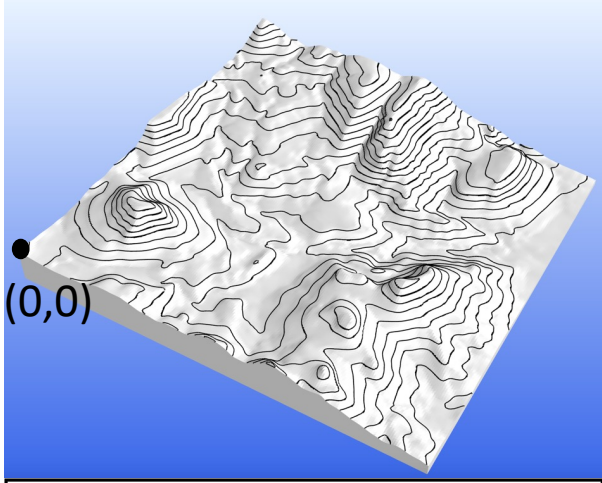

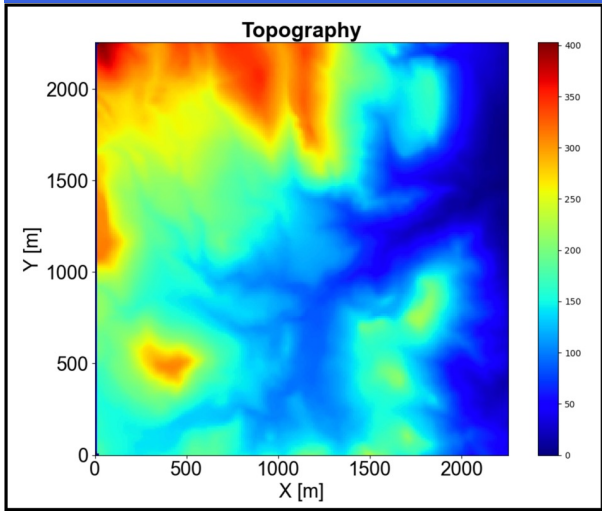

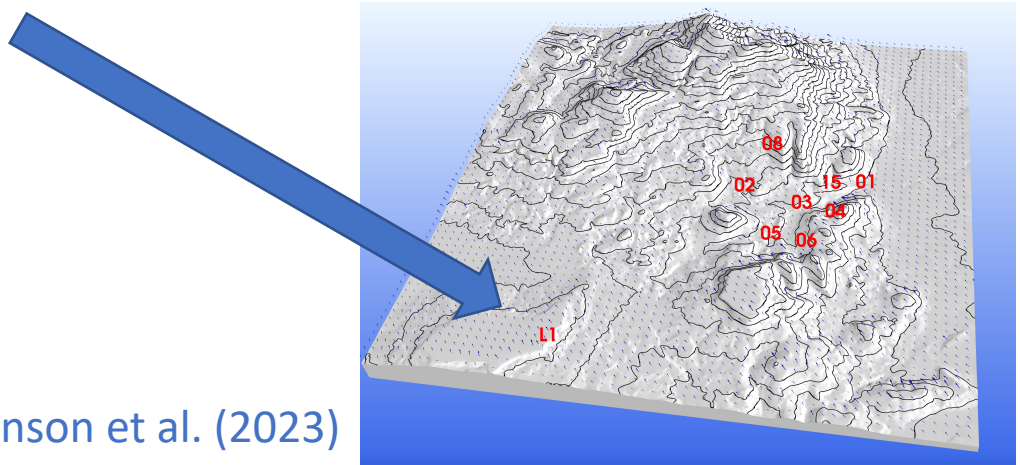

Robinson et al. (2023)

Socorro Mountains Model Results

Robinson et al. (2023)

~12 seconds to compute on laptop

Socorro Mountains Time: 2019-11-04/19:40:00

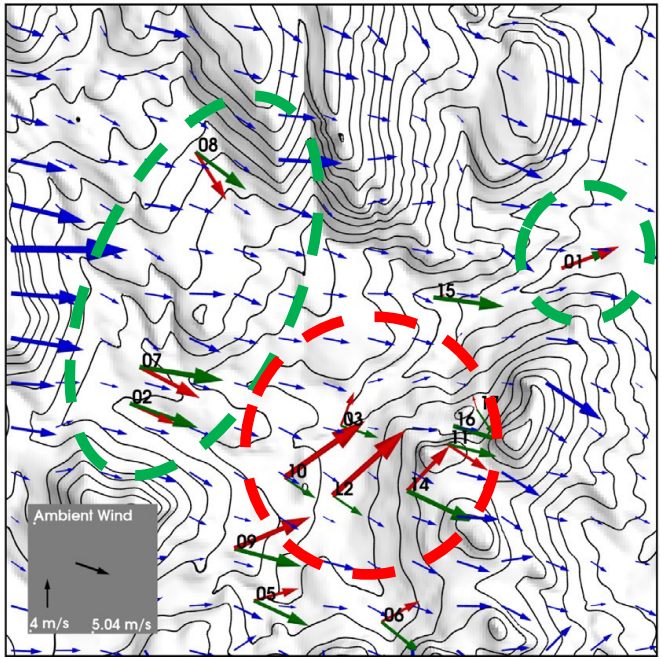

Socorro Mountains Time: 2019-11-05/12:30:00

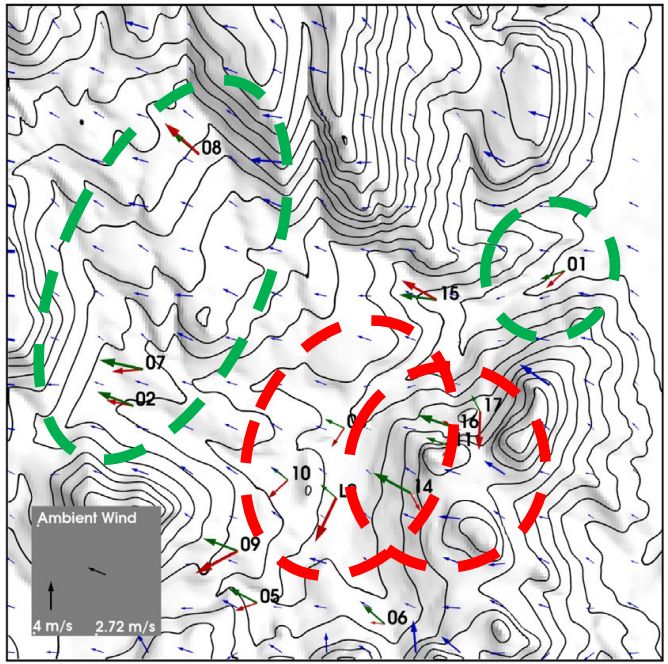

Model Winds at Sensor Location (2x Scale) Sensor Measurements (2x Scale) Model Winds

Terrain-Following QUIC-URB Conclusions

- Performs well for stagnation and speed-up of winds on upwind side of terrain features.
- Overpredicts winds on leeward side of slopes
- Cannot capture momentum and thermodynamic driven flows:
  - Canyon/Drainage flows
  - Wake eddies
  - Flow separations

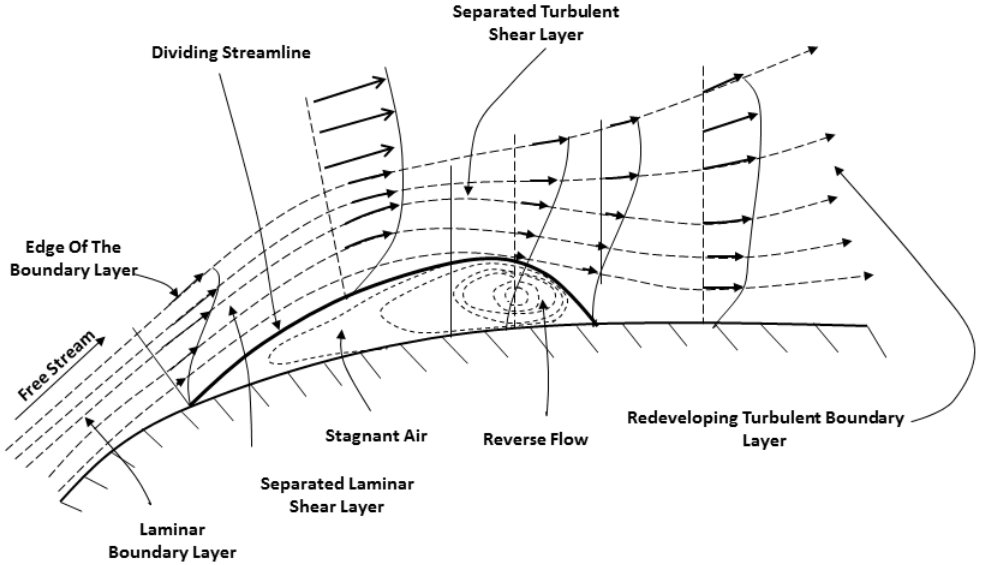

(Horton, 1968)

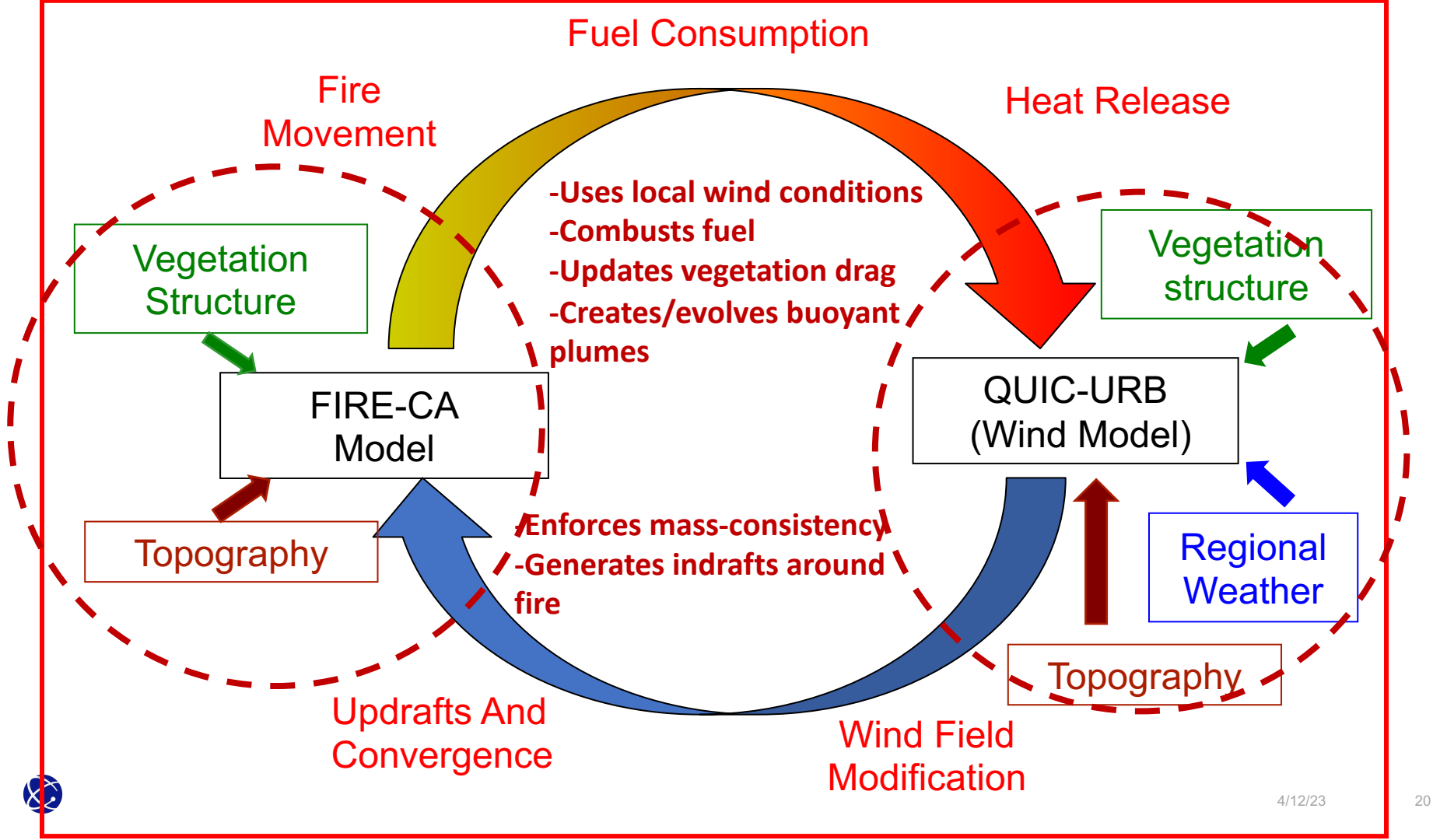
Fuel Consumption
Fire Movement
Heat Release
-Uses local wind conditions
-Combusts fuel
-Updates vegetation drag
-Creates/evolves buoyant plumes
Vegetation Structure
Vegetation structure
FIRE-CA Model
QUIC-URB (Wind Model)
Topography
-Enforces mass-consistency
-Generates indrafts around fire
Regional Weather
Topography
Updrafts And Convergence
Wind Field Modification

QUIC-Fire Brief Overview

- Discretizes energy release from combusting fuels into energy packets (EP) and calculates trajectory based on local wind conditions.
  - Turbulence and fuel drag approximations.
  - Depending on where EPs land they can:
    - Dry fuel
    - Combust dry fuel
    - Generate buoyant updrafts

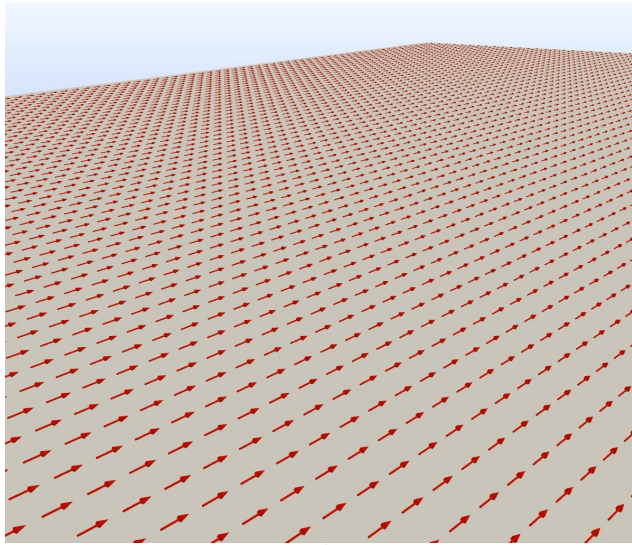

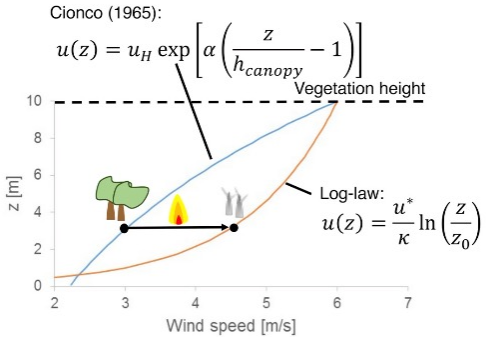

- Buoyant plume model
  - Uses Briggs theory from Davidson (1989)
  - QUIC-URB mass-conservation generates indrafts.

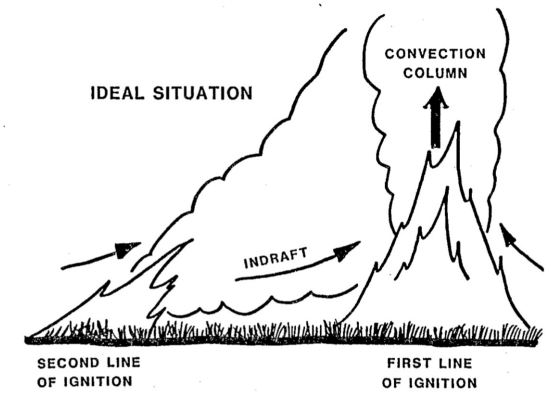

Rothermel (1984)

Terrain-Following QUIC-URB in QUIC-Fire

- Description of required changes to the code to correctly incorporate the terrain-following winds.
  - Only looking at the effect of terrain-influenced winds on fire spread in QUIC-Fire.
- Comparison of 10 simulations with FIRETEC.
  - Identical topographies.
  - Close to identical fuels.
- Identify where the code can improve.
- The following has been submitted to Environmental Modelling & Software journal under the title “The Effect of Terrain-Influenced Winds on Fire Spread in QUIC-Fire”.

Fuel Grid and Wind Grid

- Fuel Grid is ‘draped’ over terrain.
  - Simplifies input generation.
- Winds from wind grid are interpolated to fuel grid cell centers for fire routine
  - Terrain following stretching makes this non-trivial.

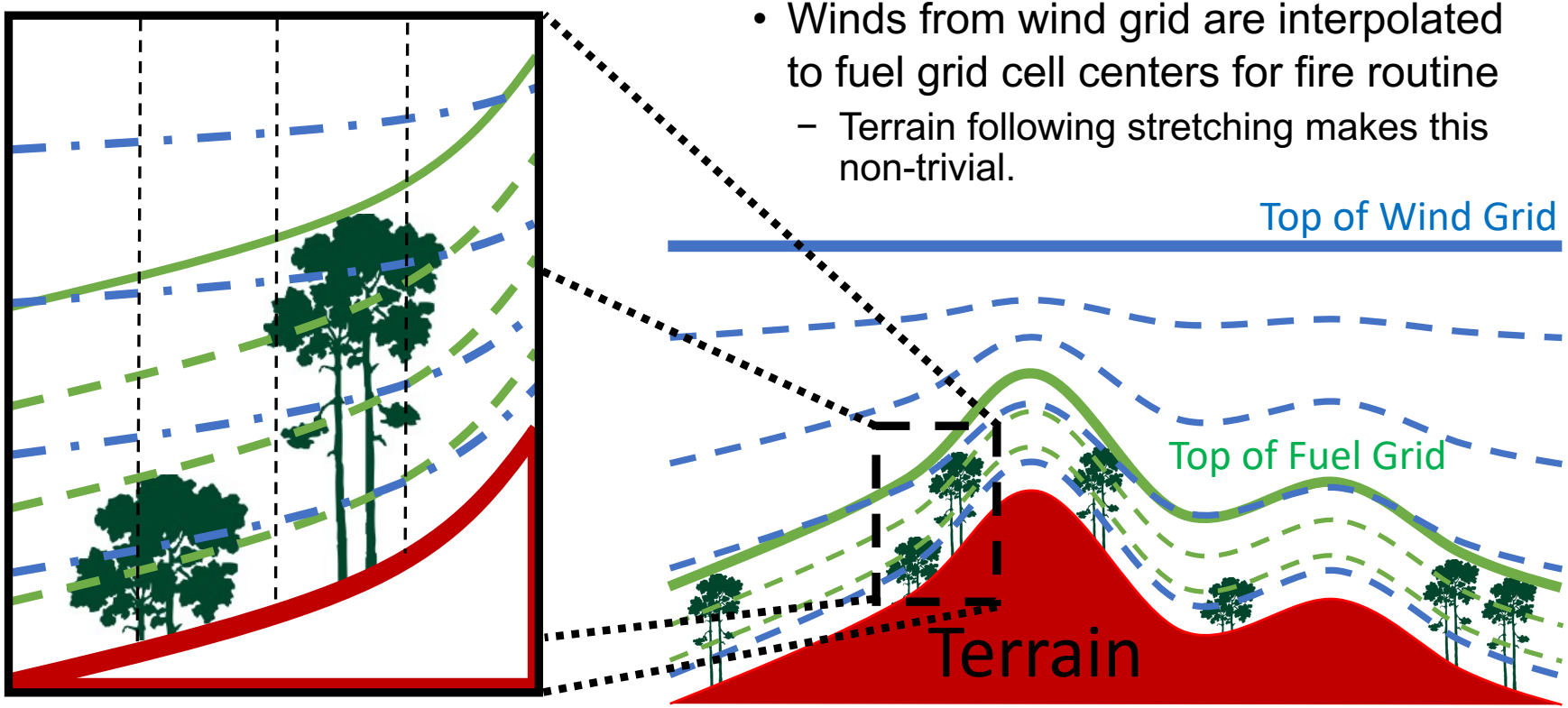

Local Surface Wind Decomposition

- Local winds for fire cells are decomposed into components:
  - Parallel to the surface: $v_{\parallel}$, v_{h_x}, and v_{h_y}
  - Perpendicular to the surface: $v_{\perp}$
- Ratio of $v_{\parallel}$ and $v_{\perp}$ determines ratio of EPs that are lofted.
- EP horizontal propagation distance scaled by $|cos\theta|$
  - θ is local elevation angle in direction of EP trajectory

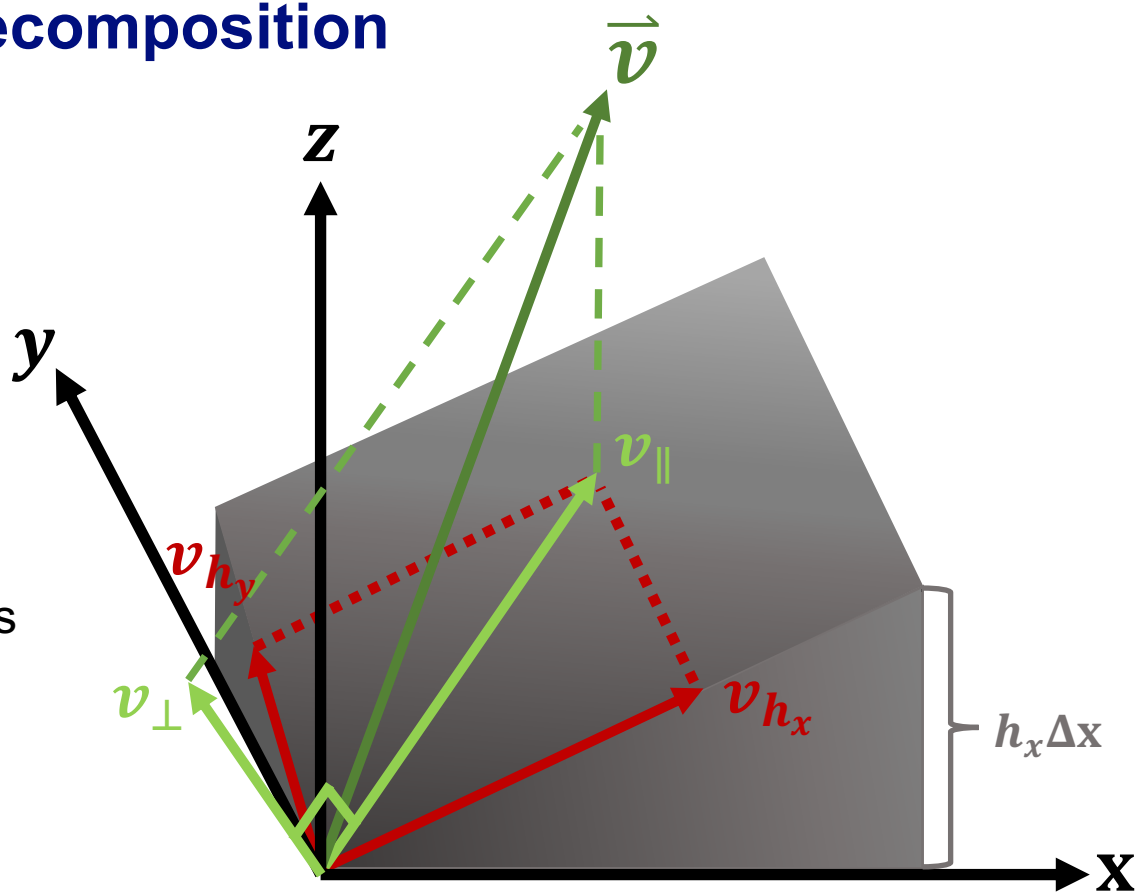

QUIC-Fire / FIRETEC Domains

- Topographies share centerline profile downwind from ignition line.
- Fuels:
  - Same generative fuels program (Trees) using identical fuel parameters.
  - Homogenous grass interfacing with Ponderosa pine forest.
  - 2 m x 2 m x 1 m fuel grid resolution
- Background win speeds: 6m/s & 12 m/s

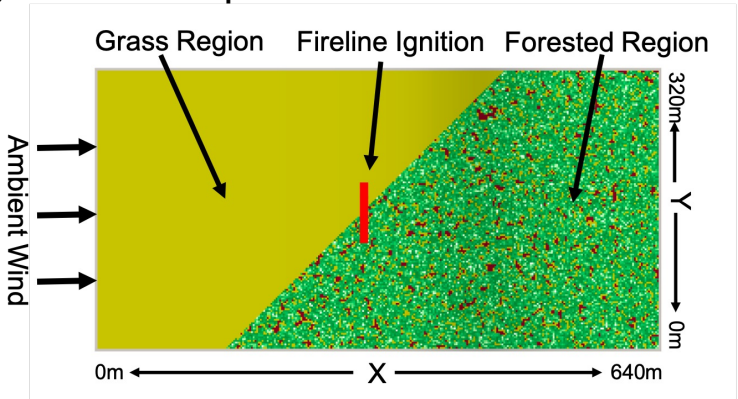

Name	Ground height (h) function	Topography
Flat	$h = 0$	
Hill	$h = base$	
Canyon	$h = \begin{cases} 55 + 40\tan^{-1}\left(\frac{\lvert x-300\rvert-140}{60}\right) & \text{for } x < 300\text{m} \\ base & \text{for } x \geq 300\text{m} \end{cases}$ Note: The elevation at the inlet wind (left) end of the topography is 103 m.	
Upcan	$h = base + \left(\frac{\lvert y-160\rvert^{1.5}}{160^{1.5}}\right) \times base$ Note: The elevation at the outlet (right) end at the corners is 211 m, or roughly double the base topography elevation of 106 m at the centerline of the outlet.	
Ridge	$h = base - \left(\frac{\lvert y-160\rvert^{1.5}}{160^{1.5}}\right) \times base$ Note: The elevation at the outlet (right) end at the corners is 1 m, or 105 m below the base topography elevation of 106 m at the centerline of the outlet.	

Fire Shapes

- 6 m/s cases for both FIRETEC and QUIC-Fire 150 seconds into simulation.

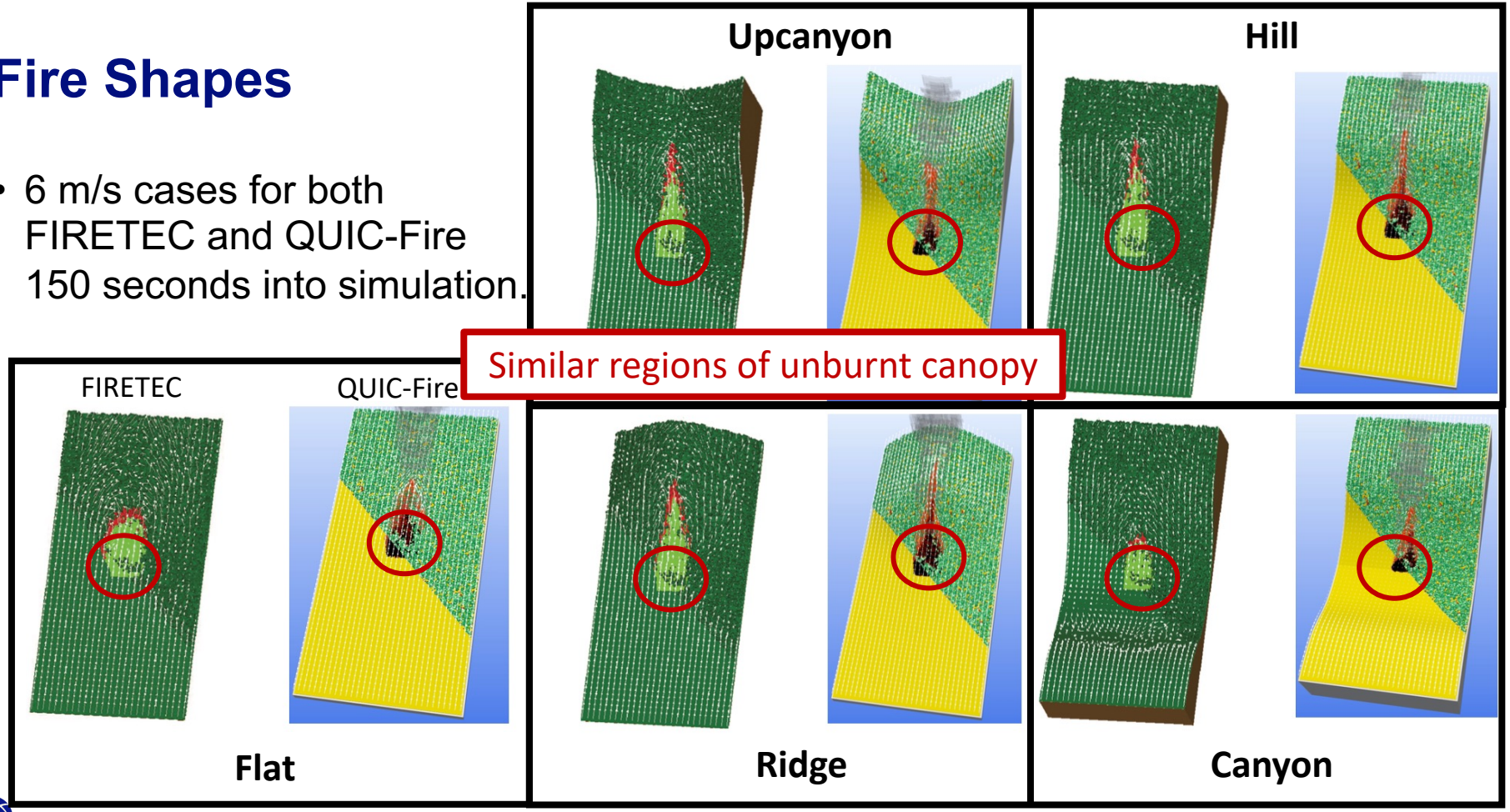

FIRETEC results from Linn et al. (2007)

Fire Shapes

- 12 m/s cases for both FIRETEC and QUIC-Fire 100 seconds into simulation.

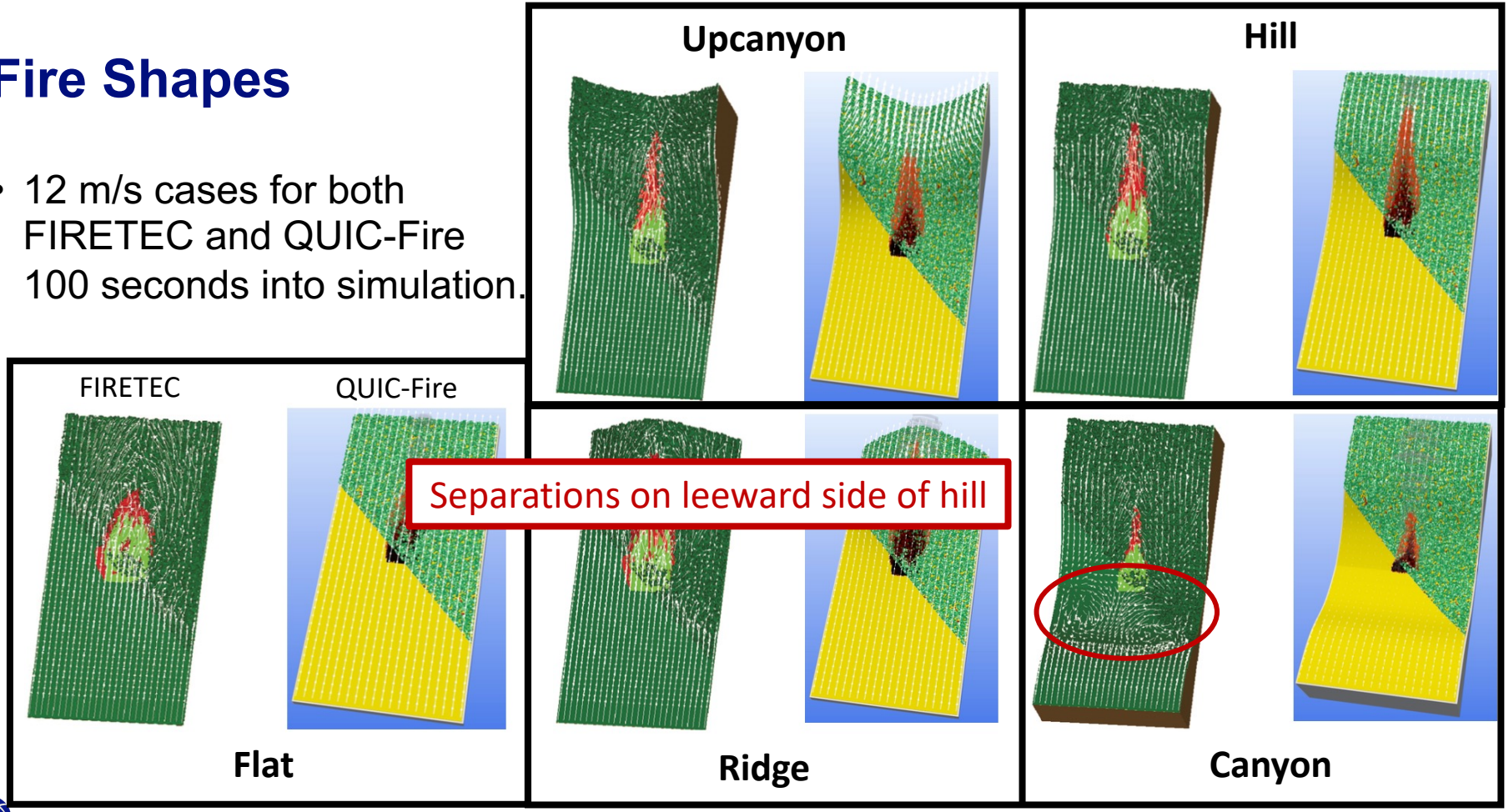

FIRETEC results from Linn et al. (2007)

Downwind Propagation Distance

- Measured using furthest downwind cell that is burning.
- Similar separation of Hill, Canyon, and Upcanyon profiles from Flat case.
- Canyon 12m/s case shows longer delay in acceleration of spread
  - Modifying flame-tilt approximation could significantly improve results.
- QUIC-Fire results lacking deceleration seen at top of terrain.
  - Missing momentum in QUIC-URB means too strong of winds at top of terrain (no separations)

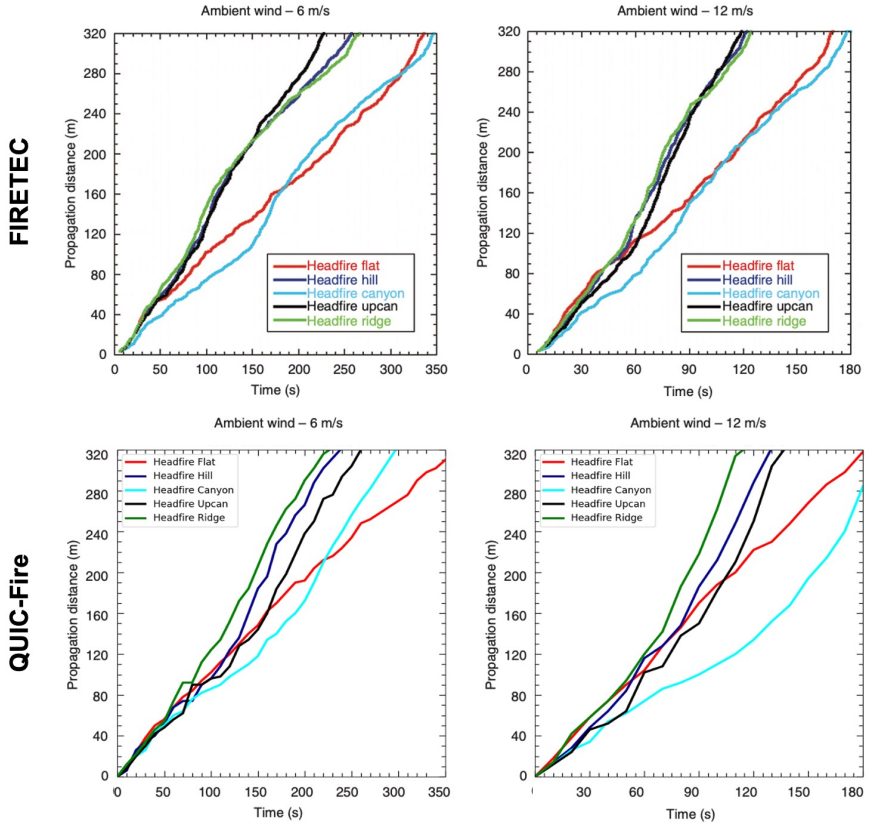

FIRETEC results from Linn et al. (2007)

Spread Rates in Regions

- Average Flat Spread Rates:

Flat Case	6 m/s	12 m/s
FIRETEC	0.8	1.8
QUIC-Fire	0.9	1.9

- Slower spread in Region 2
- Faster spread in Region 3

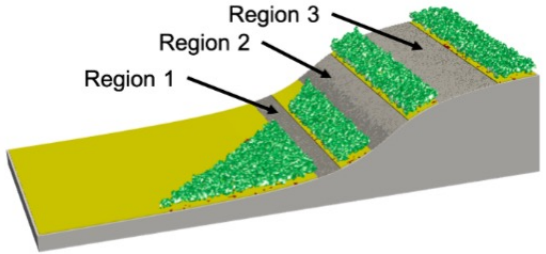

Spread rate within selected regions (ms^{-1})						
	Region 1 $40 \leq x \leq 70$ m		Region 2 $110 \leq x \leq 160$ m		Region 3 $200 \leq x \leq 280$ m	
Cases	FIRETEC	QUIC-Fire	FIRETEC	QUIC-Fire	FIRETEC	QUIC-Fire
Flat6	0.7	1.0	0.8	1.0	0.9	0.7
Hill6	1.1	1.3	2.1	1.7	1.0	1.8
Canyon6	0.7	0.8	1.9	1.0	0.8	1.5
Upcan6	1.0	0.9	2.1	1.3	1.3	1.6
Ridge6	1.3	1.3	2.3	1.4	0.9	1.7
Flat12	2.1	1.8	1.4	2.1	1.9	1.7
Hill12	2.3	1.8	3.8	2.0	2.9	3.5
Canyon12	1.1	1.3	2.8	1.4	1.6	3.1
Upcan12	1.8	1.2	4.0	2.2	3.4	4.2
Ridge12	2.3	1.6	3.4	2.8	2.1	4.2

FIRETEC results from Linn et al. (2007)

Lateral Spread

- ‘Left’ – Positive y-direction
  ‘Right’ – Negative y-direction
- Narrow Canyon spread
- Significant lateral spread to the left missing for Flat and Ridge cases.
  - QUIC-Fire doesn’t capture effect of fuel interface on background winds.

Simulation	left extent lateral spread rate (ms^{-1})		Right extent lateral spread rate (ms^{-1})	
	FIRETEC	QUIC-Fire	FIRETEC	QUIC-Fire
Flat6	0.22	0.076	-0.036	-0.082
Hill6	0.058	0.025	-0.013	-0.05
Canyon6	0.026	0.007	0.001	-0.007
Upcan6	0.039	0.023	-0.013	-0.038
Ridge6	0.086	0.052	-0.037	-0.070
Flat12	0.46	0.10	-0.29	-0.20
Hill12	0.23	0.107	-0.18	-0.169
Canyon12	0.024	0.032	0.027	-0.053
Upcan12	0.14	0.108	-0.15	-0.20
Ridge12	0.47	0.182	-0.25	-0.20

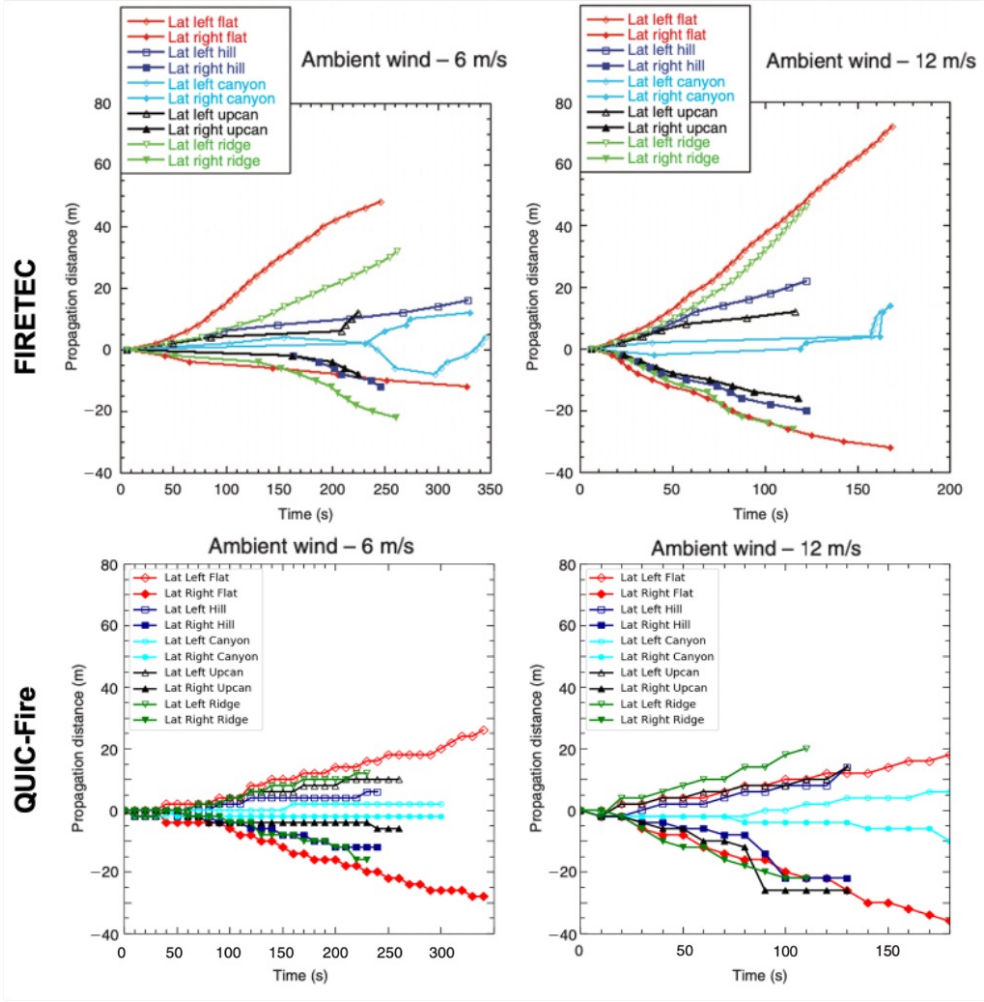

FIRETEC results from Linn et al. (2007)

Conclusions

- Terrain-influenced winds from QUIC-URB show a step in the right direction for capturing fire behavior on terrain.
  - Similar separation of propagation rates due to terrain.
  - Similar lateral spread distance (especially Canyon case).
- Not captured:
  - Acceleration of fire spread in steepest portions.
  - Response to fuel interface.
    - Lack of increased ‘Left’ lateral spread observed in FIRETEC results.
  - Deceleration as terrain slopes approach zero.
    - Possible missing flow separations

Some Details of the SOR Algorithm in QUIC-FIRE

- The λ matrix used for calculating the mass-conserved wind field is reset to zero each timestep.
  - Reasoning: Plume segments move each timestep so the indrafts move also.
- The SOR algorithm is iterated 10 times each timestep.
  - Reasoning: Increase speed of the code (not much adjustment is seen after 10 iterations).
- Each SOR iteration for each cell only references nearby cells.
- An adaptive window is used in QUIC-Fire that calculates the mass-consistent wind field in a 10 cell buffer around the extent of the plumes and fire.
  - Reasoning: Speeds up code and no reason to calculate mass conserved winds beyond that point.

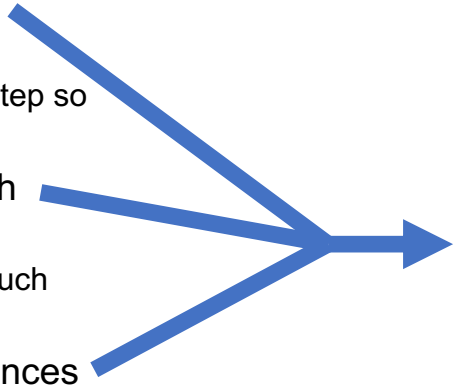

Plumes have a maximum influence range of 10 cells.

Modification to SOR

- What if λ matrix is not reset each timestep?
  - Will it make a difference?
  - Will it create persistent artifacts?
  - Will it introduce substantial errors to the wind field?
  - Will there be boundary effects?

Dots are fires varying from 50-330 MW

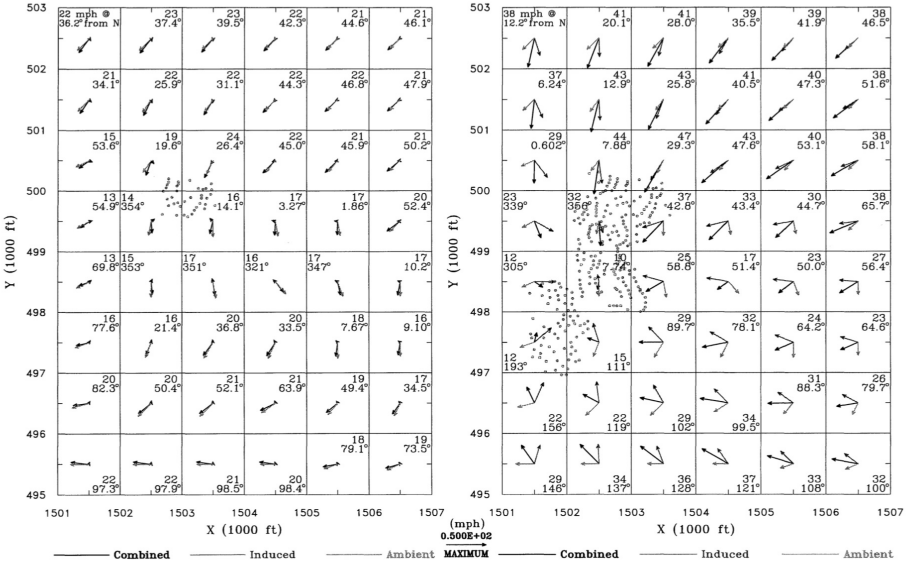

FIGURE 3: Horizontal induced winds @ 20 m, 1145 a.m. ± 5 min. The dotted circles indicate all 38 of the 50 MW fires that are driving the flow. So few fires barely affect the prevailing wind.

FIGURE 4: Horizontal combined winds @ 20 m, 1200 p.m. ± 10 min. 259 fires are burning at rates which vary from 50 to 330 MW. Now that the fire has grown in strength, the magnitude of the fire-induced winds is comparable to that of the ambient.

Trelles et al. (1997)

Buoyant updrafts have been observed generating indrafts from much farther than 20 m (2 m * 10 cells).

Changes in Fire-Fire Interactions

Ring Fire

Spot Fires

Line Fires (Wind Aligned)

λ set to Zero

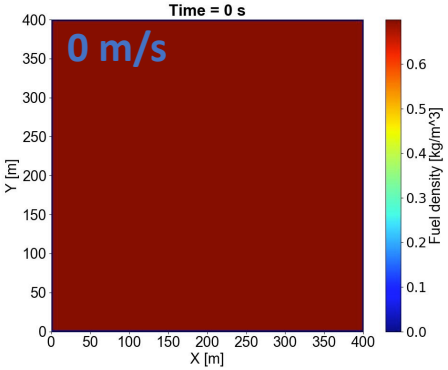

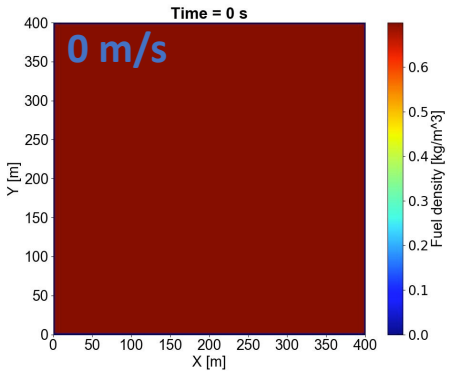

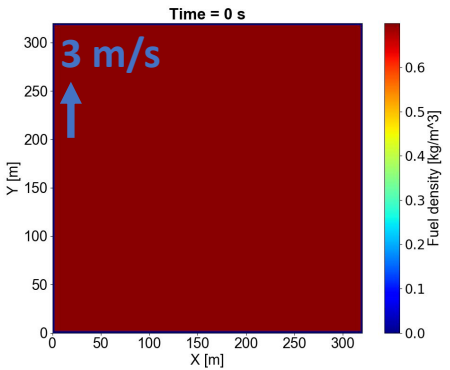

Prev. λ Used

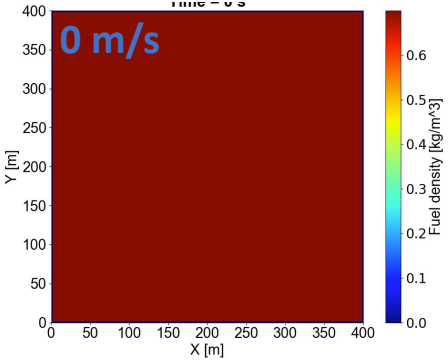

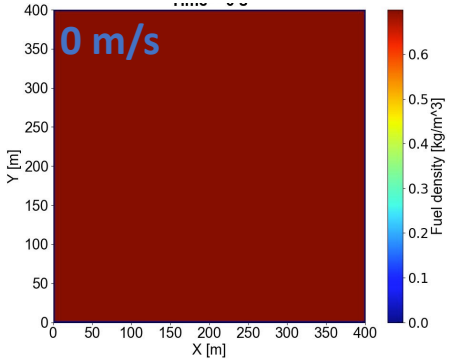

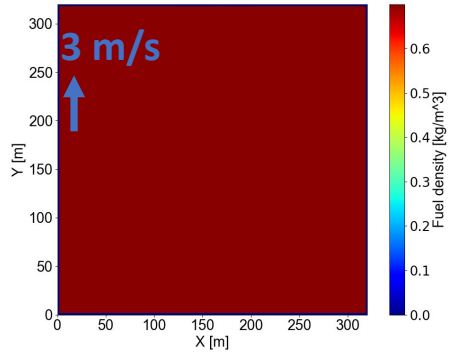

Head Fires Preserved

- Doesn't change fire phenomenology already captured in QUIC-Fire.

3 m/s background wind

λ set to Zero

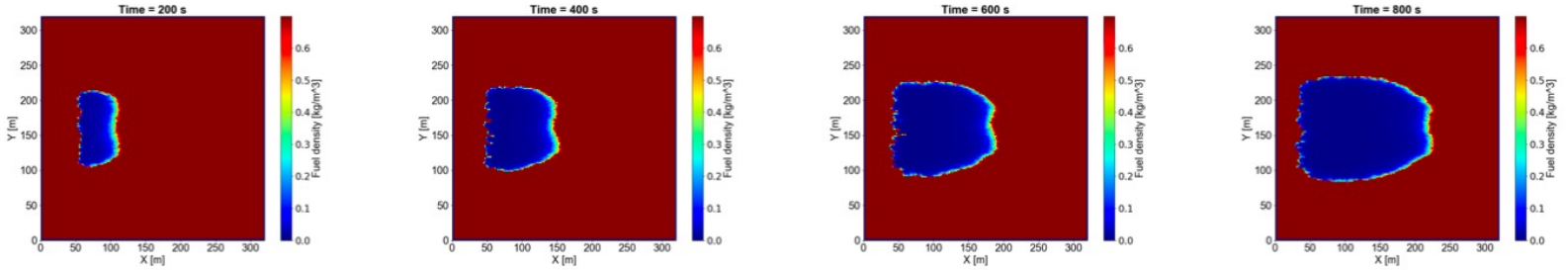

Prev. λ Used

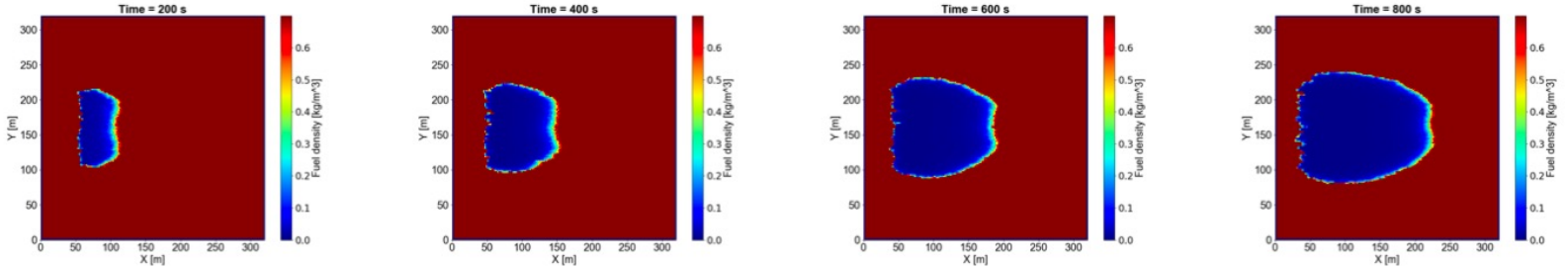

Persistent Artifacts?

- Error formed by comparing:
  - 10 iteration solution that keeps previous λ
  - 1,000 iteration solution with λ set to zero each timestep.
- Multiple plumes interacting.
- Error decays and no artifacts generated.
- Largest errors limited to top of domain.

Plume structure shown in dark blue

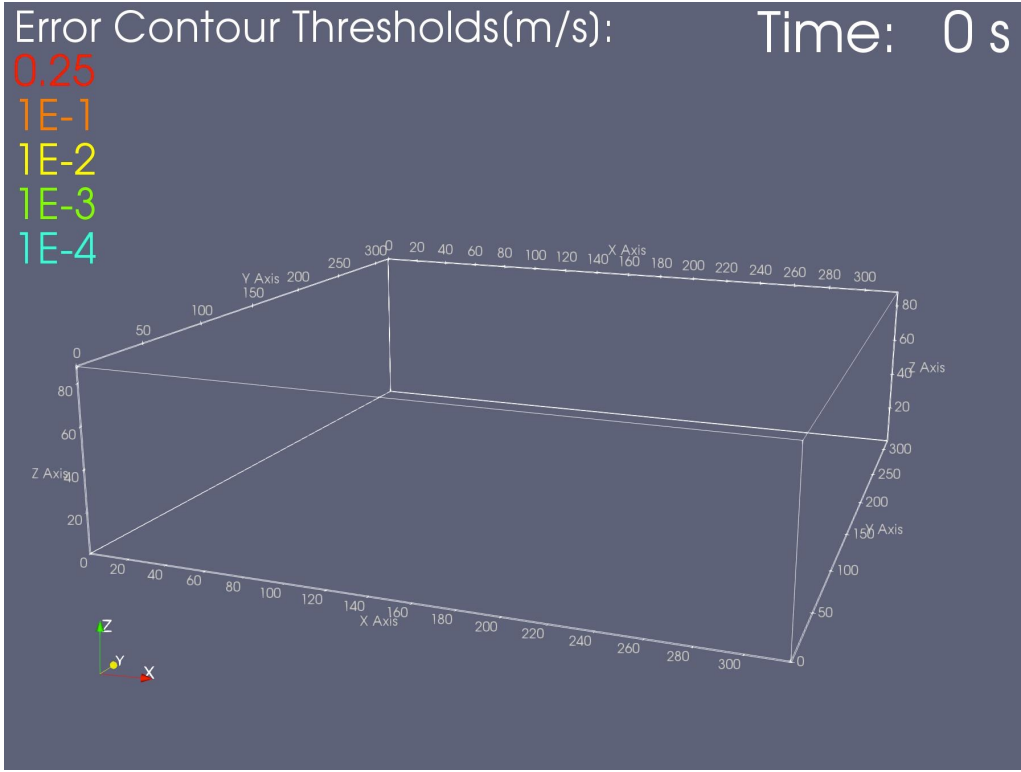

Boundary Effects?

- Head fire case with multiple buffer (σ) sizes.
  - Ran in parallel to avoid random variation.
- Errors:

$$L_1 = \frac{1}{N} \sum_{i=i_{Start}}^{i_{End}} \sum_{j=j_{Start}}^{j_{End}} \sum_{k=k_{Start}}^{k_{End}} \left|u_{i,j,k} - u_{i,j,k}^{True}\right| + \left|v_{i,j,k} - v_{i,j,k}^{True}\right| + \left|w_{i,j,k} - w_{i,j,k}^{True}\right|$$

$$\text{and } L_{\text{inf}} = \max\left(\left|u_{i,j,k} - u_{i,j,k}^{True}\right| + \left|v_{i,j,k} - v_{i,j,k}^{True}\right| + \left|w_{i,j,k} - w_{i,j,k}^{True}\right|\right)_{i,j,k}$$

$$i_{start} = i_{min} - \sigma \text{ and } i_{end} = i_{max} + \sigma$$

- Smaller buffer is better.
- Max errors comparable to original method.

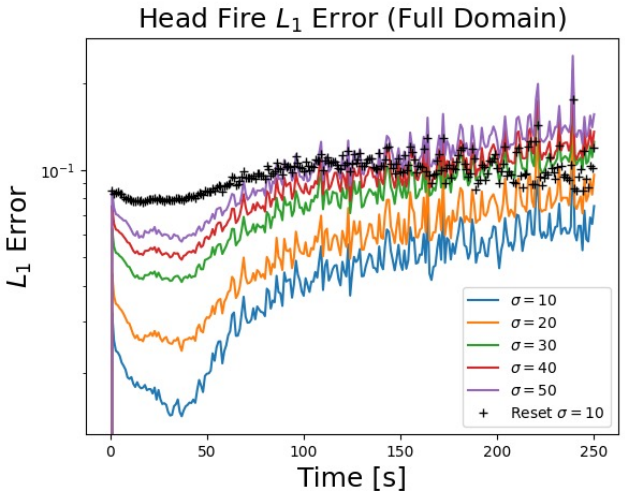

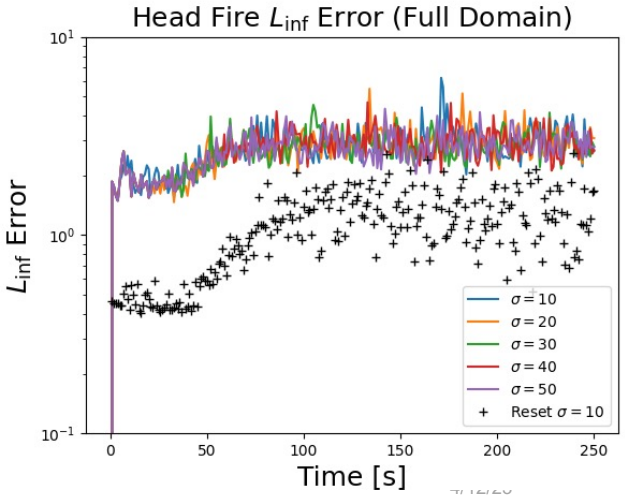

SOR Modification Conclusions

- New fire phenomenology captured in model.
  - No added computational cost.
- No added artifacts and comparable maximum error.
  - Global error actually improved in some cases.
- Important for prescribed fire safety.

Prescribed Fire Ignition Techniques

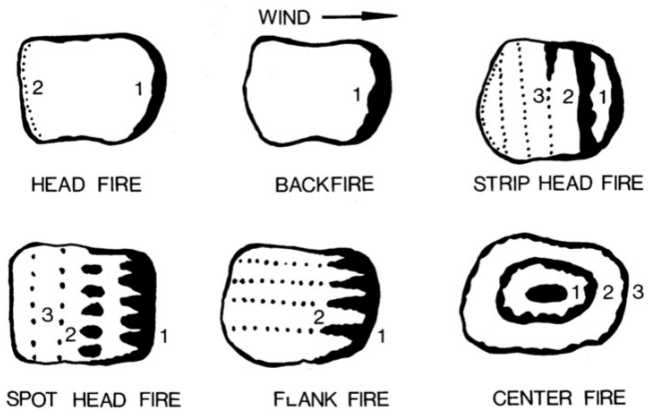

Martin and Dell (1978)

Future Directions

- GPU implementation of SOR solver.
- Map QUIC-URB building wake parameterizations to terrain-following coordinates.
- Sub-grid flame tilt modifications.
- Modifications to fuel drag scheme.

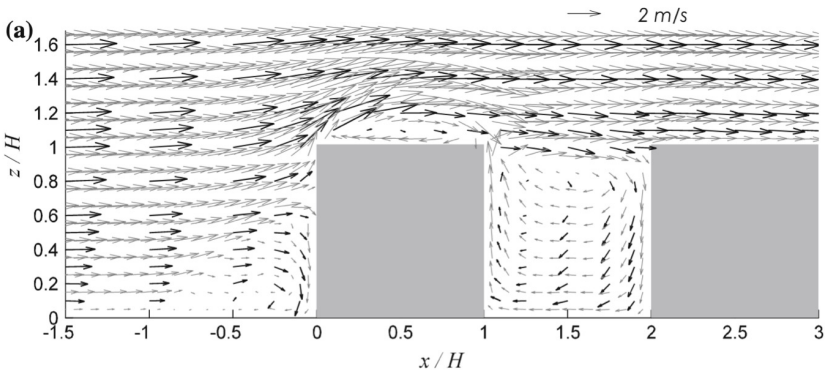

QUIC-URB Wake Parameterizations

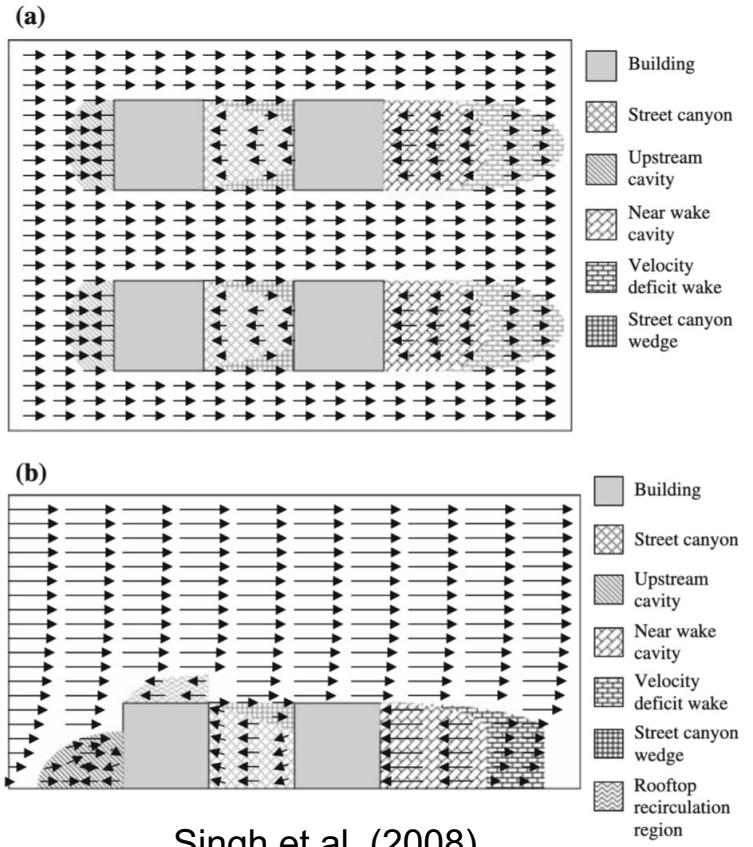

Singh et al. (2008)

Thank You!

Kevin Speer

Fred Huffer

Family

Friends

FSU Students

FSU Faculty

LANL Colleagues

External Colleagues

Bryan Quaife

Rod Linn

Neda Yaghoobian

Kevin Hiers

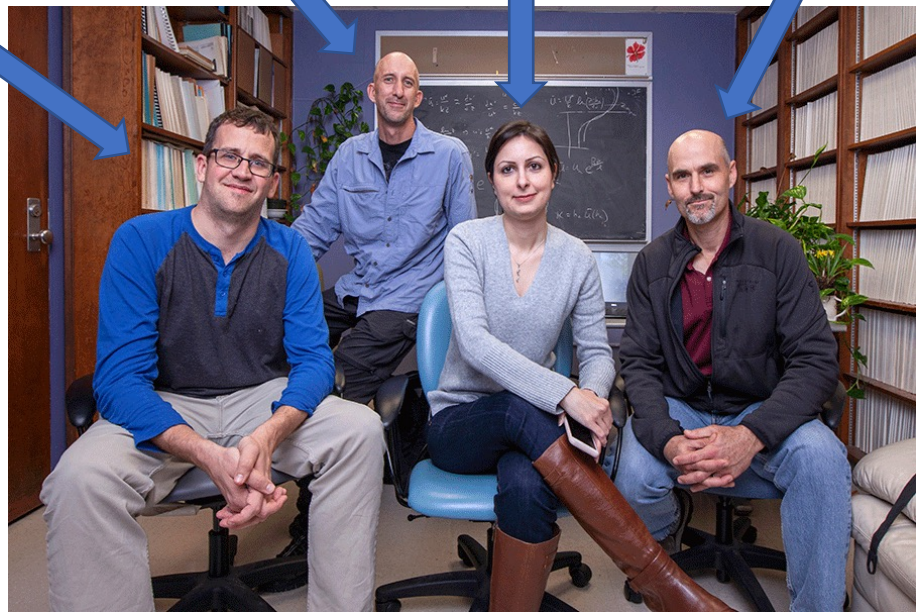

Mark Wallheiser Copyright: © 2019 FAMU-FSU College of Engineering

Funding & Support

LANL LDRD

USFS

Southern Research Station

Rocky Mountain Research Station

SERDP

Questions?